IMPACT ON CERAMIC ARMOR SEAMS

Timothy G. Talladay, Frederick C. Rickert
US Army Tank-Automotive Research, Development and Engineering Center

SUMMARY

Ceramic armor provides unique opportunities to achieve lighter weight protection of tactical vehicles. However ceramics are much more sensitive to multi-impact damage than traditional metallic armors. Small ceramic tiles are generally used, and the intersecting locations of these tiles are well known to provide reduced protection relative to the center of a tile. For armor panel assembly, it is useful to know how the width of the intersection correlates with reduced performance. Experiments and simulations to determine if a critical point exists in the performance relationship. No critical point was found, and the relationship was effectively linear.

INTRODUCTION

Ceramic-based armor systems are increasingly used in lightweight vehicles for protection. The attractiveness of these systems is that they tend to yield more mass efficient armors than, for example, a monolithic piece of armor-grade steel. Most published work to date has focused on the effect of center impact rather than edge impact. This situation is reasonable because there is still much debate over what properties are indicative of an efficient armor ceramic; for example see a recent article by Krell and Strassburger [1]. In assembly of a real armor panel, ceramic tiles with small lateral dimensions, in comparison to the overall area that must be covered, are used in order to increase multi-hit effectiveness [2 - 3]. However, the presence of multiple small ceramic tiles inherently creates gaps between the tiles, called seams. The presence of these seams is well known to cause reduced armor performance. During manufacturing, the width of these seams is monitored or controlled. It is desirable to know if a critical point exists in the armor performance curve as a function of seam width. If such a critical point exists then a compromise can be made between seam width and other metrics such as the multi-hit performance, i.e. reducing adjacent tile damage, or the cost of manufacturing controls.

Furthermore, it is desirable to be capable of simulating impact on an armor panel. The goal of simulations is predictive capability that would reduce physical testing. However, this goal still seems to be reasonably far away since “calibration” of simulations by comparison to actual tests has been and is still necessary. The capability to perform design iterations to narrow the experimental scope, even if the results are not precisely accurate but indicate the correct trends, is useful. Furthermore, if the physical basis of the model is correct, models are immensely helpful for understanding why a phenomenon occurs during a ballistic event.

Therefore, the first purpose of this study was to determine the ballistic performance of the seam between two adjacent tiles as a function of seam width. It was anticipated that a critical point would exist at which ballistic performance would precipitously decrease for an increase is seam width. The second purpose of the study was to perform computational simulations of the same event and compare the simulations to the experiment. The desire of this work would be that the simulations replicate the experiments and provide insight into the mechanics of the event.

EXPERIMENT

Test samples were assembled with AD-90 (90% purity) alumina ceramic tiles manufactured by CoorsTek (Golden, Colorado). The square tiles had a nominal thickness of 7.874 mm and a side length of 101.6 mm. The tiles were bonded to 6.35 mm thick 6061-T6 aluminum plates with rectangular dimensions of 304.8 x 152.4 mm. The ratio of thicknesses was selected based on the work of Hetherington [4]. The aluminum plate was prepared by cleaning with acetone and sanding to roughen the surface. The adhesive was a five minute epoxy manufactured by ITW Devcon (Danvers, Maryland). The two part epoxy was mixed, and a small amount was applied to the entire surface of the ceramic tile. The first tile was pressed onto the aluminum plate and rotated in small-angle oscillations to spread and remove excess epoxy. The minor amounts of excess epoxy were removed from the periphery of bond. The tile was firmly held in place, compressing the tile against the aluminum. A second tile was added similarly after the epoxy was fully cured. The distance between the two tiles was controlled by precision machined steel gauges placed between the two tiles. After the epoxy cured, the gauges were removed. The result was an unfilled seam between two alumina tiles backed by an aluminum plate (see Fig. 1). The seam widths were varied in 0.635 mm intervals from 0.0 mm (intimate contact) to 2.54 mm. It must be noted that due to variations in the perimeter surfaces of the tiles, the 0.0 mm seam had small variations; however, it was the smallest seam width that could practically be achieved.

The projectile utilized in the experiment was an L/D 3 conical-nosed rod, adapted from Anderson et al. [5] and similar to that of Wilkins et al. [6]. The projectile was AISI 4340 steel heat treated to a hardness of Rockwell C 53 ± 2. The actual diameter of the body was 7.57 mm. The overall length was 22.86 mm with a nose length of 7.62 mm. The average projectile weight was 6.18 g. A small skirt on the base of the projectile engaged the rifling in the launcher barrel. The projectile was fired from a fixed mount launcher. The propellant charge was varied in order to achieve the desired impact velocity.

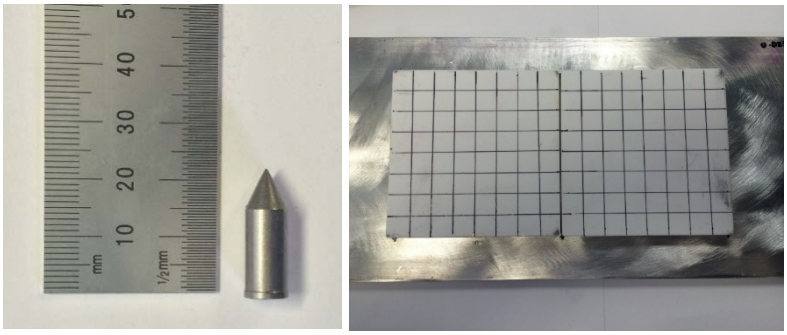

Figure 1. Projectile and alumina-aluminum panel. There is a 12.7 mm grid drawn on the ceramic plates to provide a reference for the high speed camera.

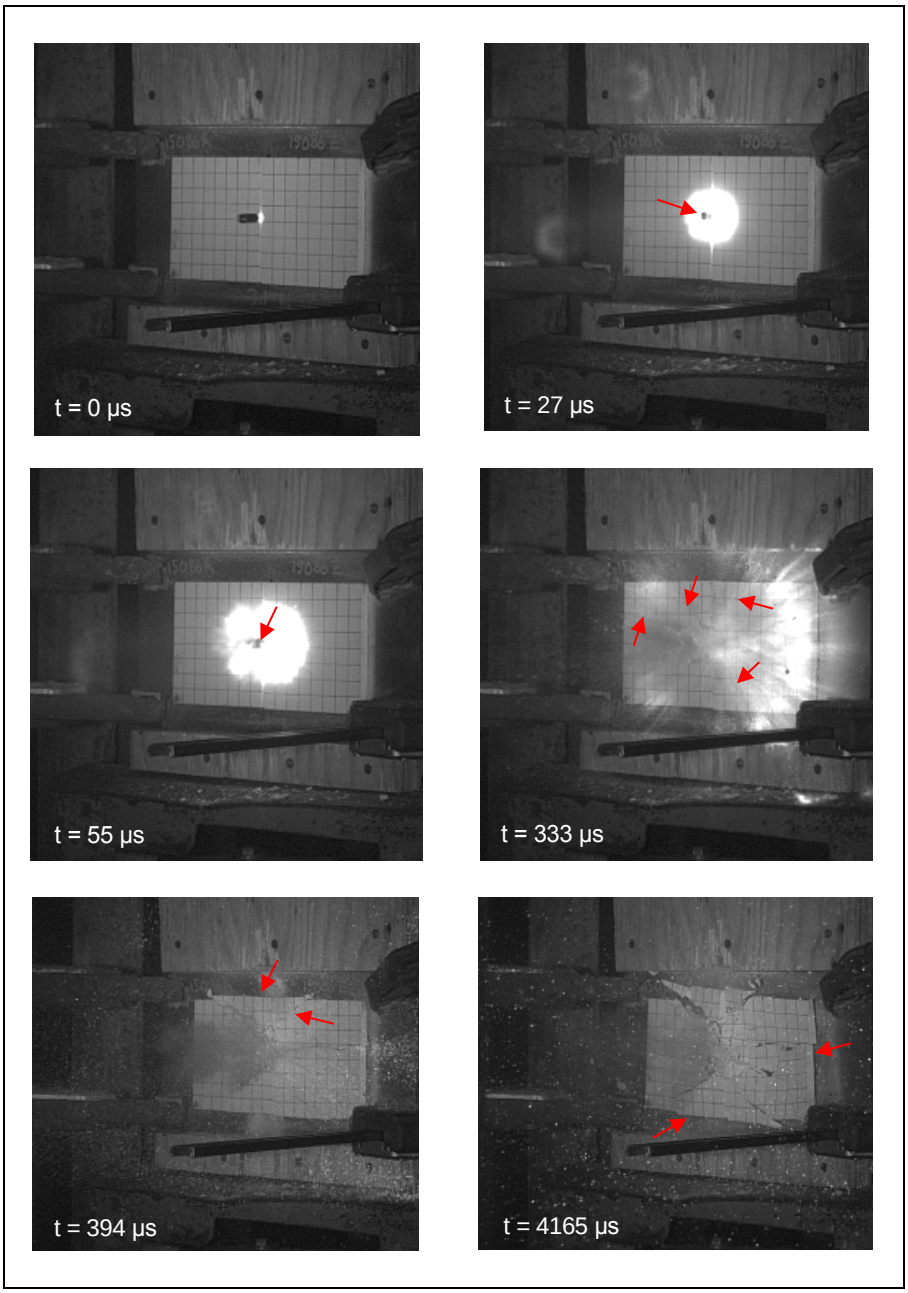

Figure 2. An example impact on the ceramic tiles. The red arrows highlight the projectile entering the seam, crack formation in the ceramic, and global motion of large chucks of fragmented ceramic.

The impact was monitored on the strike face by a Vision Research Phantom V411 high speed camera at 36,000 frames/s (see Fig. 2). Residual velocity was monitored by a Phantom V1610 at 19,000 frames/s. Two-shot V_{50} ballistic limits were calculated for each seam width configuration. Residual velocity as a function of impact velocity was calculated as well and a fit to the Lambert-Jonas equation was obtained. The desired impact point was the center of the seam between the two ceramic tiles. Fair impacts were judged by the precision of the impact on the seam. Occasionally, a projectile departed from the intended flight path and yielded an invalid impact. A coarse assessment as to

monitor for a projectile which impacted visibly off the seam. For finer assessment, the cracking and fragmentation of the ceramic was monitored. If the fragmentation was noticeably asymmetric, the impact was discounted due to a likely off-seam impact. Residual velocity of a projectile that exited the sample was measured using the high speed camera setup previously described. Utilizing this method, residual velocity was determined as a function of impact velocity. This data is hereafter referred to as V_S-V_R.

$$V_R = \begin{matrix} 0 & , V_S \leq V_L \\ a(V_S^p - V_L^p)^{1/p} & , V_s > V_L \end{matrix} \quad (1)$$

The V_{50} results are given in Table I. At 0.0 and 2.54 mm seam widths, the separation between the two shots used to calculate the V_{50} were too great. US Army Test Operations Procedure 2-2-710 prescribes a maximum difference of 18 m/s for calculation of a two-shot V_{50}. However, during the experiment, importance was given to obtaining a bound for V_{50} then ensuring sufficient samples for populated V_S-V_R data. The experimental V_{50} and Lambert-Jonas model agreed well, differing at most by 2.2%.

In order to make results scalable for other projectile sizes and seam widths, the performance was normalized. The performance of each seam was normalized by the ballistic limit velocity (BLV) of the 0.0 mm seam. The seam width was normalized by the projectile diameter.

$$Normalized\ BLV = \frac{V_{BL,w=x\ mm}}{V_{BL,w=0.0\ mm}} \quad (2)$$

$$Normalized\ Seam\ Width = \frac{w}{d_p = 7.57\ mm} \quad (3)$$

The normalized BLV as a function of the normalized seam width is linear (see Figure 3). The slope of the line is approximately negative one. This response was not expected; a more complex relationship was anticipated.

Table I. Ballistic limits for seam panels.

Seam Width, mm	Experimental (two shot)			Lambert-Jonas Fit
	V_{50}, m/s	Highest Velocity Non-Perforation, m/s	Lowest Velocity Perforation, m/s	V_L, m/s
0.0	810	795	824	817
0.635	752	748	756	736
1.27	652	656	649	655
1.905	630	628	633	615
2.540	533	521	546	529

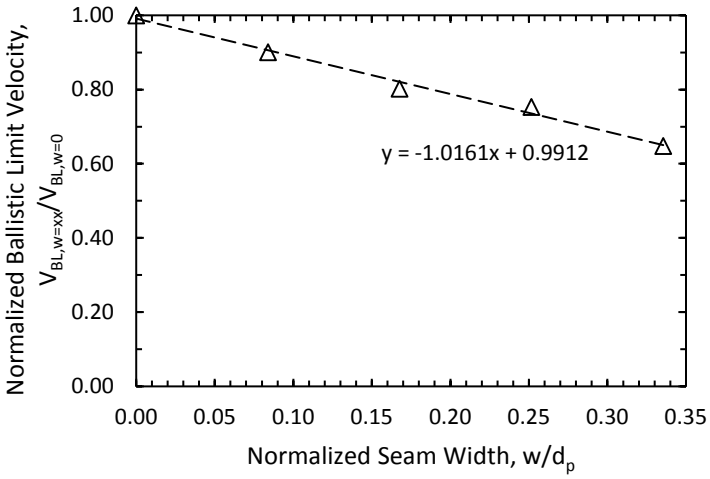

Figure 3. Normalized ballistic limit velocity as a function of normalized seam width.

Figure 4. Damage to a projectile that was arrested in the aluminum backing plate. The impact was on the 2.54 mm seam at a velocity of 483 m/s. The residual projectile length is 18.5 mm.

The 0.0 mm seam resulted in the most severe damage to the projectile and was the most likely to erode or heavily fracture the projectile body. At 824 m/s, the projectile appeared to be completely consumed in the impact. No chunks of intact projectile perforated the plate; only debris perforated the plate. The perforation hole was still large in diameter relative to the projectile diameter. Progressively with accompanying increased seam width, the projectile damage shifted predominantly toward damaging the nose while leaving the body intact. Finally, the 2.54 mm seam resulted primarily only in damage to the tip of the projectile.

The seam width between the alumina tiles affected the failure of the back plate. Non-perforating impacts near the BLV resulted in local deformation and radial cracking on the distal side of the aluminum plate. For the 0.0 mm seam, the failure was observed as the formation of a large plug which opened and broke away from the impact site. The area of plastic deformation that was loaded by a fractured cone of ceramic, as described by the Florence model, was substantially greater than the projectile diameter.

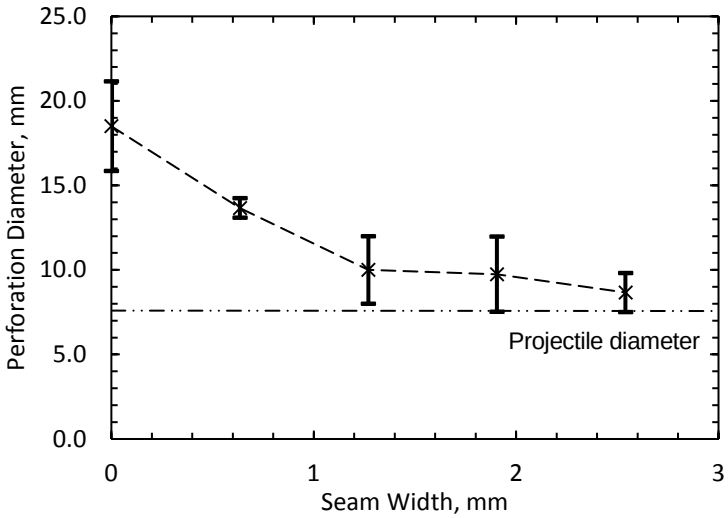

Figure 5. Perforation diameter decreased as seam width increased.

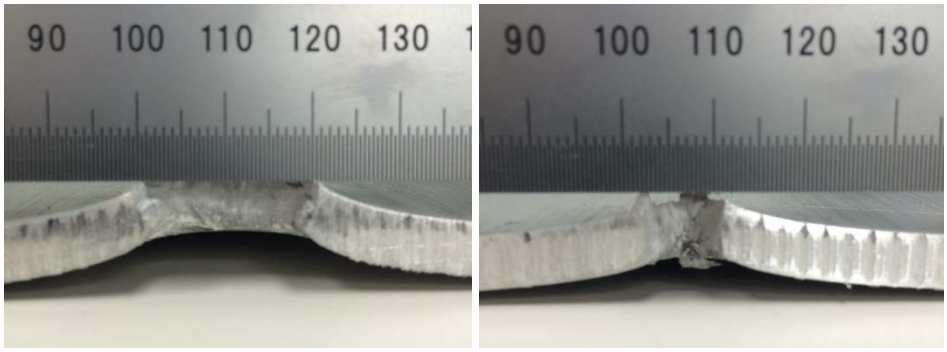

Figure 6. Characteristic failures of 0.0 mm and 2.54 mm seams.

SIMULATION

The simulations were conducted in the hydrocode Elastic Plastic Impact Calculations (EPIC). The simulation was performed in three-dimensional half symmetry. The EPIC short form was used to define node geometry of bricks, and each brick was divided into 24 tetrahedrons. The plane of symmetry was through the axis of the seam. The nodal spacing in the projectile was constant. The nodal spacing of the ceramic and aluminum was equivalent to the projectile's spacing for three projectile radii. Outward from three radii, the nodal spacing expanded in order to reduce computational burden.

The Johnson-Cook model was used for both the steel and the aluminum. Material constants are given in Ref. [5] and [7]. Constants for the 90% alumina for the improved Johnson-Holmquist ceramic model (JH-2) were not available and had to be estimated from experimental data [9 – 12]. Simulations were also compared to literature data for much higher velocity impact of Ref. [13] in order to avoid calibrating the model to the impact conditions described in this manuscript.

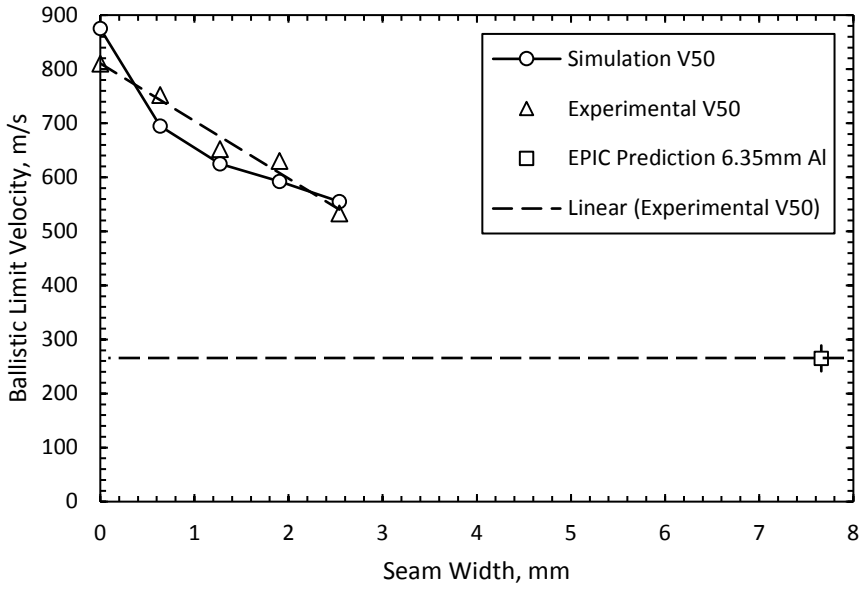

Figure 7. Comparison of ballistic limit values from experiment and simulation.

Figure 7 displays a plot of the V_{50} values from the experiment and simulation. Solid connecting lines were included in the plot to make a trend apparent. A linear fit line was applied previously to the experimental data, however a linear fit did not seem appropriate for the simulation results. The solid connecting segments between the simulation values appeared to suggest a more complex trend. EPIC was used to predict the performance of the 6.35 mm thick aluminum backing, which would be the point at which the seam width is equal to the projectile diameter. Logically this point would be the asymptote which the performance curve would approach. If the range of investigation in the seam width were extended further, it is anticipated that a more complex relationship between seam width and ballistic performance would exist. However, such wide seam widths are not practical in armor design and thus were not further investigated.

Residual velocity was tracked in the simulations in order to compare to the experiments. Figure 8 displays the residual velocity as a function of impact velocity. Because the BLV values calculated by simulation were in error relative to the experiments, the residual velocities also appeared incorrect. In order to assess the accuracy of residual velocity prediction, the V_{50} of each seam simulation was adjusted to be equal to the experimental V_{50} for that seam. This adjusted impact velocity is displayed in Figure 9. With the simulation V_{50} corrected to match the experiment, the V_S-V_R curves match quite well. For the 1.27 mm seam, the experimental response was more variable. In some instances, the projectile nose fractured (data points above the L-J fit line); in others, the body fractured (data points below the L-J fit line). These changes in mass and fracture likely caused changes in exit response and residual velocity. The simulation results match quite well with the fractured nose response observed in the experiment. Small variations in impact locations may be able account for the variation in projectile fracture.

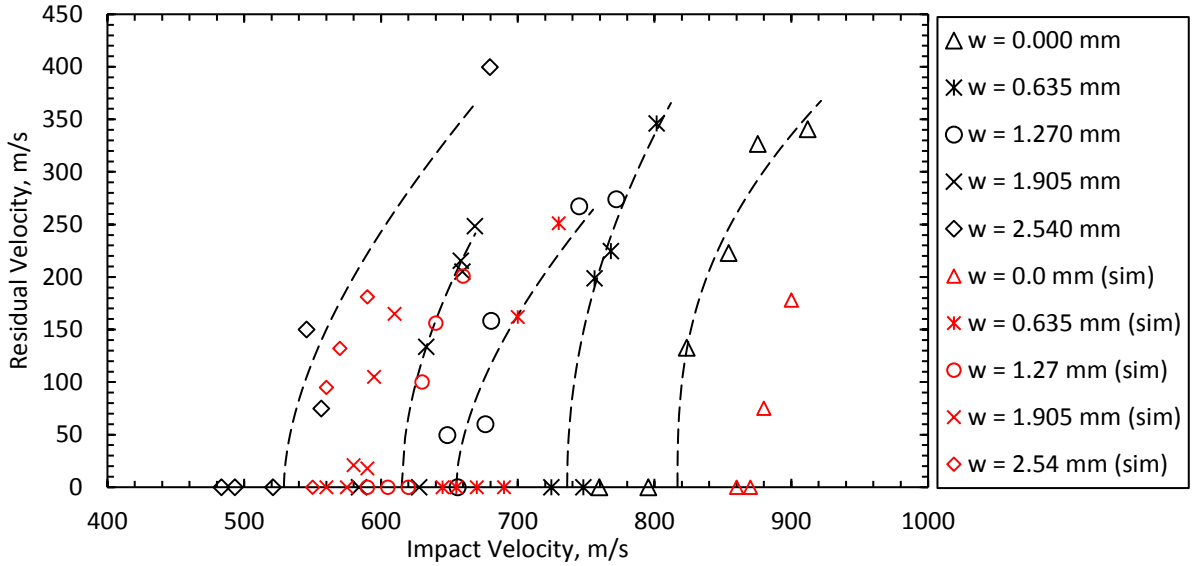

Figure 8. Comparison of residual velocity data for experiment and simulation.

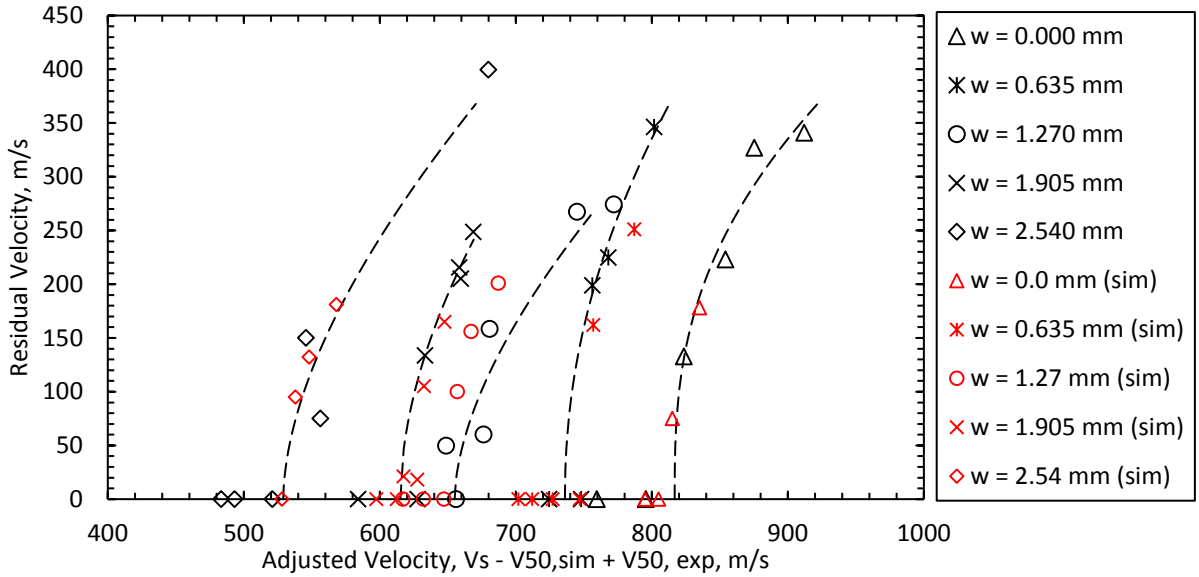

Figure 9. Residual velocity data corrected for V50 error.

The failure process is shown in Figure 10 for impact near the ballistic limit velocity. The geometry column is later in time than the damage column. The damage column is displayed at earlier time to show the incipient failure of the aluminum plate that preceded the geometry shown at 125 μs. The failure of the 0.0 mm seam appears to be driven by tension-shear resulting in thinning followed by plug failure of the aluminum due to the blunted projectile and large cone of ceramic. Progressively, the failure changes. For the 2.54 mm seam, the failure appears to be much more of a traditional ductile hole growth and distal surface fracture associated with aluminum.

Seam Width, mm	Velocity, m/s	Damage at 63 µs	Geometry at 125 µs
0.0	880	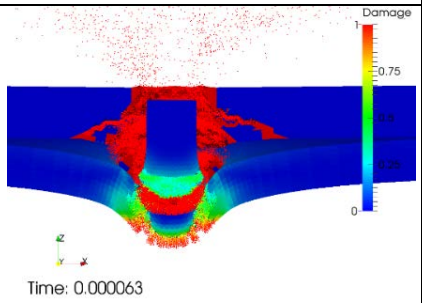	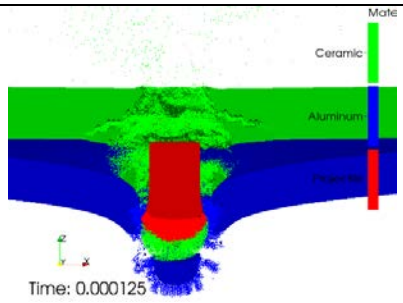
0.635	726	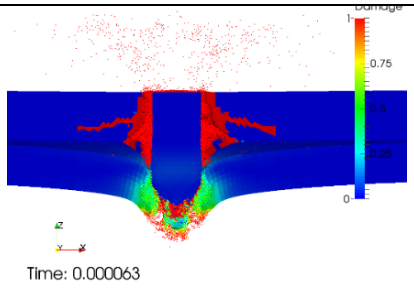	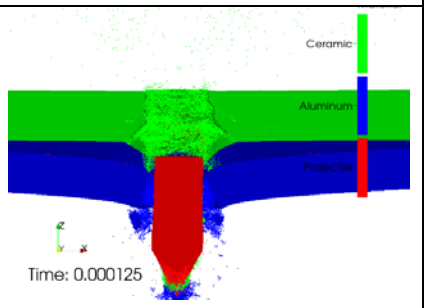
1.27	630	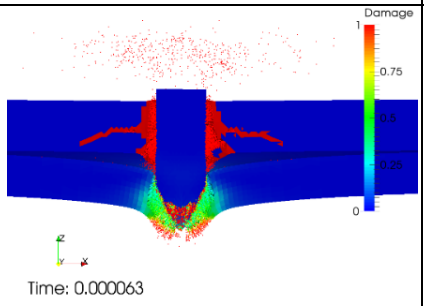	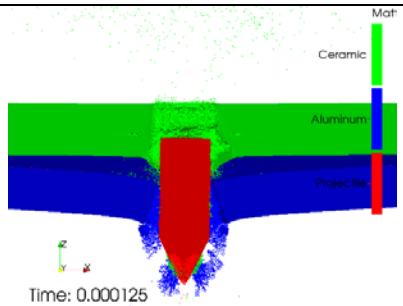
1.905	610	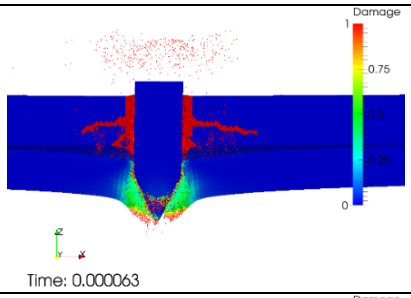	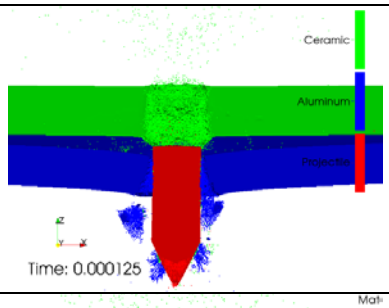
2.54	560	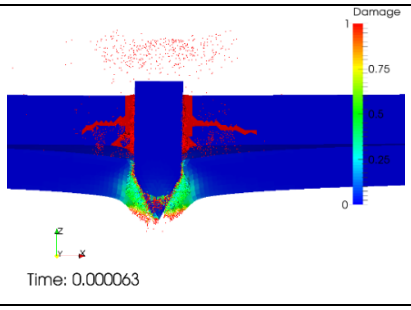	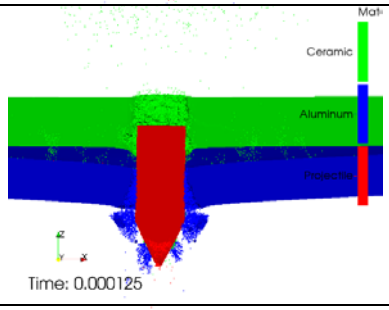

Figure 10. Failure of aluminum backing plate for each seam configuration.

CONCLUSION

It was anticipated that a critical point would exist at which ballistic performance would precipitously decrease for an increase is seam width. However, no such point was found within the bounds of the experiment. The ballistic performance, judged by the ballistic limit, decayed linearly with increasing seam width. The gradient of the relationship is approximately negative one. The simulations compared well to the experiments and aided in understanding the process of failure of the aluminum backing plate. As the seam width was increased, the damage to the projectile was reduced and the failure of the aluminum backing plate changed from a tensile-shear failure to primarily tensile failure. The conclusion of these results is that the armor developer must investigate other effects, such as multi-impact performance or manufacturing cost that are associated with arrayed armor performance, in order to develop a compromise in design.

REFERENCES

[1] A. Krell and E. Strassburger, "Order of influences on the ballistic resistance of armor ceramics and single crystals," *Mater. Sci. and Eng. A*, vol. 597, pp. 422-430, 2014.

[2] W. S. de Rosset, "Patterned armor performance evaluation," *Int. J. Impact Eng.*, vol. 31, pp. 1223-1234, 2005.

[3] P. J. Hazell and M. Moutinho, "The Design of Mosaic Armour: The Influence of Tile Size on Ballistic Performance," *Materials and Design*, vol. 29, pp. 1497-1503, 2008.

[4] J. G. Hetherington, "The Optimization of Two Component Composite Armors," *Int. J. Impact Engng*, vol. 12, no. 3, pp. 409-414, 1992.

[5] C. Anderson Jr, C. Weiss and S. Chocron, "Impact experiments into borosilicate glass at three Scale sizes," *J. Appl. Mech.*, vol. 78, pp. 051011-1051011-10, 2009.

[6] M. L. Wilkins, C. F. Cline and C. A. Honodel, "Fourth progress report of the light armor program," University of California, Livermore, 1970.

[7] T. Holmquist, D. Templeton and K. Bishnoi, "Constitutive modeling of aluminum nitride for large strain, high strain rate, and high pressure applications," *Int. J. Impact Eng.*, vol. 25, pp. 211-231, 2001.

[8] S. J. Bless and D. L. Jurick, "Design for multi-hit capability," *Int. J. Impact Eng.*, vol. 21, no. 10, pp. 905-908, 1998.

[9] CoorsTek, "Ceramic armor data sheet," 2013. [Online]. Available: http://www.coorstek.com. [Accessed 10 Dec 2013].

[10] J. Ning, H. Ren and P. Li, "Mechanical behaviors and damage constitutive model of ceramics under shock compression," *Acta Mech. Sin.*, vol. 24, pp. 305-315, 2008.

[11] A. M. Rajendran, "High strain rate behavior of metals, ceramics, and concrete," US Air Force (Wright Laboratory report WL-TR-92-4006, WPAFB, 1992.

[12] Z. Rosenberg, "On the relation between the Hugoniot elastic limit and yield strength of brittle materials," *J. Appl. Phys.*, vol. 74, pp. 732-753, 1993.

[13] C. Anderson, "Ballistic performance of confined Al2O3 ceramic tiles," *Int. J. IMpact Eng.*, vol. 12, no. 2, pp. 167-187, 1992.